IMPLEMENTATION OF FUZZY BASED POWER CONTROL OF BDFIG WITH SUPER-TWISTING SLIDING MODE CONTROL

R. Durga Rao

Asst. Professor & Head, Department of EEE.JNTUH COLLEGE OF ENGINEERING MANTHANI.

durgarao@jntuh.ac.in

ABSTRACT: The super twisting sliding mode direct power control (SSM-DPC) strategy for brushless doubly fed induction generator (BDFIG) is the proposed method in this paper. Direct power control suffers from active and reactive power ripples and current distortions, which corrupt the quality of output power. The SSM-DPC strategy controls active and reactive power directly without the need of phase locked loop. Moreover, its transient performance is similar to DPC and its steady state performance is the same as vector control. The fuzzy controller is used to remove the above defined harmonics and to improve the performance of the proposed model. The proposed controller is robust to uncertainties toward parameter variations and achieves constant converter switching frequency, by using space vector modulation. Simulation results BDFIG are provided to validate the effectiveness, correctness and the robustness of the proposed strategy.

I. INTRODUCTION

Brushless doubly-fed induction generators (BDFIG) have shown promising prospect as an alternative to the conventional doubly-fed induction generator (DFIG) in commercial wind turbine applications especially for offshore wind farms, since it does not require brushes and slip-rings (as the name implies) which results in higher reliability and lower maintenance cost operations [1-3]. Another member of the doubly-fed machine family, BDFIG inherits all the advantages of the conventional DFIG and has been regarded as a viable replacement [3-6]. The BDFIG with nested-loop/wound rotor consists of power-stator, rotor, and control-stator windings, as depicted in Fig.1.

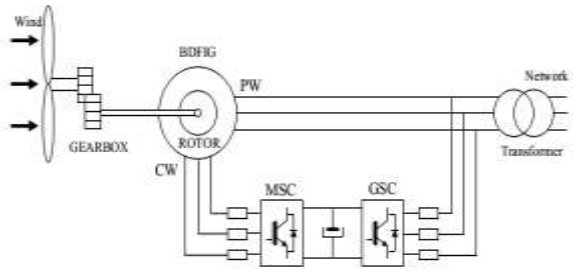

Fig. 1 A generic conceptual diagram of the BDFIG system for adjustable speed constant frequency grid-connected applications

The power winding (PW) is directly connected to the grid, while control winding (CW) is supplied via a fractionally-rated dual-bridge converter in 'back-to-back' configuration for bi-directional power flow [4]. Controller designs for the BDFIG are somewhat difficult to implement which could be down to the model complexities yielding to complex structure caused by the inner rotor loop (presence of the rotor resistance), heavy parameter dependence, large number of degrees of freedom and multiple-input/multiple output [5], thus appropriate BDFIG control strategies are very demanding but highly required. Vector control (VC) is a common and practical scheme pertinent to induction machines is also applied to the BDFIG [6, 7]. Sensitivity to parameter variation, detuning effect of PI controllers, deficiency during grid disturbances and necessity of position sensors are accounted as the main drawbacks of BVC.

Efforts towards prominent brushless doubly fed reluctance generator (BDFRG) have been carried out to conquer these drawbacks [8, 9], which could potentially be applicable universally to the BDFIG with minor adjustments. As an alternative to VC, the

direct torque control (DTC) [10] and direct power control (DPC) [11], are proposed for the BDFIG. Such strategies have fast dynamic response, simple implementation and robustness. The DTC/DPC provides direct regulation of the machines torque/power by selecting proper voltage vectors from the lookup-tables. However, converter switching frequency varies with operating conditions, which results in large torque/power ripples and current distortions. To improve such shortcomings, while keeping the advantages of DTC/DPC over the VC, the sliding-mode control (SMC) is proposed for induction machines [12] and DFIGs [13]. The SMC is a robust control method for nonlinear systems with large perturbations and parameter variations [14]. The SMC has been proposed to control the DFIG under non-ideal grid voltage conditions [15, 16].

The application of SMC for BDFIG in [17], illustrates the robustness of this method against parameter variations. Advantages of the SMC are the simple implementation, disturbance rejection, strong robustness, and fast dynamic responses. However, its stabilization time is not necessarily finite and undesired chattering appears on the controlled states. To overcome these drawbacks, forms of internal-SMC are proposed for DFIG, which delivers smooth active power to an unbalanced grid with minimized torque/power ripple [18]. However, this method requires a discrete control action, which requires high switching frequency for applying the control output via the inverter. Alternatively, the second-order sliding mode does not have a discrete output and mitigates the chattering [19, 20], in the presence of disturbances and model inaccuracies.

Thus, the second-order SMC suffers from complex mathematical calculations and its implementation is difficult when the state variables are increased [14]. The integral-SMC for BDFIG is improved by means of boundary layer and feed-forward terms but make the controller sensitive to parameter variations, while the control output is not discrete and provides fast dynamic response [21]. Super-twisting is a recently developed theory in the SMC design, which is proven to be efficient for electromechanical systems [22]. In the light of the latest development in the field, this paper proposes a super-twisting sliding-mode direct power control (SSM-DPC) for controlling active and reactive power of BDFIG, without using inner current loop regulator and phase-lock loop (PLL).

The main advantage of super-twisting SMC is that it only requires a sliding surface functions (S) and not its derivative (dS/dt) [23]. This controller mitigates the chattering that exists in most SMC strategies, while keeping SMC excellent static/dynamic performances and robustness, in case of uncertainties and parameter variations. The transient performance of the proposed strategy is similar to DPC and its steady-state performance is comparable to VC. Rest of the paper is organized as follows. Dynamic modelling of the BDFIG and configuration is presented in Section II. Super-twisting SMC technique is introduced, whilst control objectives of sliding variables, and controller design of the proposed SSM-DPC are constructed in Section III. Comparative qualitative and quantitative results are presented in Section IV, which confirms the feasibility and efficiency of the proposed controller. Simulation of 2 MW and experimental verification of a 3 kW BDFIG are presented and outlined in Section V. Finally, Section VI draws conclusions.

II. BDFIG DYNAMIC MODEL AND CONFIGURATION

The BDFIG consists of a complicated mathematical model and structural arrangement due to existing of voltage sources and resistances in its rotor loop. In order to design a controller for the BDFIG, the model complexity needs simplifying. In [10], a dynamic model of BDFIG is presented in rotor reference frame, which resembles close alignments to DFIG equivalent circuit depicted in Fig. 2.

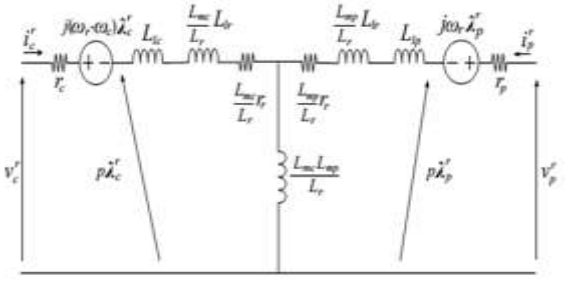

Fig. 2. Representation of the BDFIG presented model.

The dynamic model equations of this BDFIG model are expressed in space-vector form as follows [10]:

$$\vec{v}_c^{\,r} = r_c\,\vec{i}_c^{\,r} + p\vec{\lambda}_c^{\,r} + j(\omega_r - \omega_c)\vec{\lambda}_c^{\,r} \qquad (1)$$

$$\vec{v}_p{}^r = r_p\,\vec{i}_p{}^r + p\vec{\lambda}_p{}^r + j\omega_r\vec{\lambda}_p{}^r \quad (2)$$

$$\vec{\lambda}_c{}^r = \left(L_{lc} + \frac{L_{mc}}{L_r}\,L_{lr}\right)\vec{i}_c{}^r + \frac{L_{mc}L_{mp}}{L_r}\vec{i}_p{}^r + \frac{L_{mc}r_r}{L_r}\int \vec{i}_c{}^r\,dt \quad (3)$$

$$\vec{\lambda}_p{}^r = \left(L_{lp} + \frac{L_{mp}}{L_r}\,L_{lr}\right)\vec{i}_p{}^r + \frac{L_{mc}L_{mp}}{L_r}\vec{i}_c{}^r + \frac{L_{mp}r_r}{L_r}\int \vec{i}_p{}^r\,dt \quad (4)$$

Due to the effect of integrators in the flux equations in (3) and (4), cannot be transformed to other reference frames as per model representation in [10], therefore, this model does not simplify the controller design. Since, the variation range of rotor-speed/CW-frequency in BDFIG is under ±30% of the synchronous speed ($\omega_e \cong 100\pi$), the variation range of the rotor frequency is $20\pi < \omega_r < 50\pi$ [10]. Therefore,

$$\frac{r_r L_{mp}}{L_{mc}+L_{mp}} \ll (\omega_e - \omega_r)L_{lp}{}',$$

$$\frac{r_r L_{mc}}{L_{mc}+L_{mp}} \ll (\omega_e - \omega_r)L_{lc}{}'$$

Consequently, resistances $r_r\,L_{mp} / (L_{mc} + L_{mp})$ and $r_r\,L_{mc} / (L_{mc} + L_{mp})$ are neglected. Neglecting those resistances makes the BDFIG model analogous to DFIG, since the proposed controller is based on SMC; it is robust to the error due to this simplification. The model is further modified by transferring to the CW reference frame depicted in Fig. 3, which its dynamic equations are as follows:

$$\vec{v}_c = r_c\,\vec{i}_c{}^c + p\vec{\lambda}_c{}^c \quad (5)$$

$$\vec{v}_p = r_p\,\vec{i}_p{}^c + p\vec{\lambda}_p{}^c + j\omega_c\vec{\lambda}_p{}^c \quad (6)$$

$$\vec{\lambda}_c = L_c{}'\,\vec{i}_c + L_m\,\vec{i}_p \quad (7)$$

$$\vec{\lambda}_p = L_p{}'\,\vec{i}_p + L_m\,\vec{i}_c \quad (8)$$

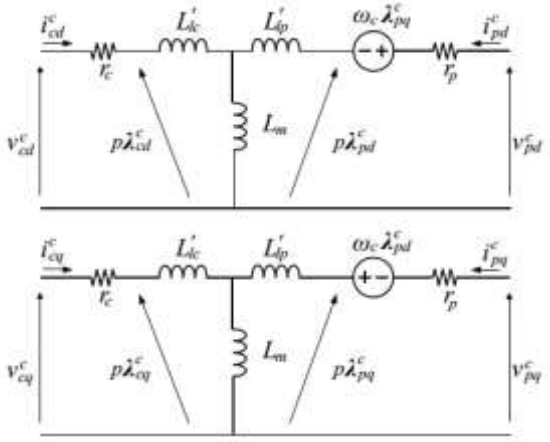

Fig. 3.Reduced dq-model of the BDFIG in the CW reference frame

According to (7) and (8), the relation between PW and CW fluxes is presented as

$$\vec{\lambda}_p = \frac{L_m}{L_c}\,\vec{\lambda}_c + \sigma L_p{}'\vec{i}_p \quad (9)$$

The model (Fig. 3) is appropriate for implementing control strategies like vector control, direct torque/power control and sliding mode control for the BDFIG.

III. SUPER-TWISTING SMC AND PROPOSED SSM-DPC STRATEGY

A. Super-Twisting Sliding Mode Control Mechanism

The main drawbacks of the traditional SMC are chattering effect and discontinuous high-frequency switching control which is impractical. To overcome these problems, super twisting controller is used. A single-dimensional motion of a unit mass system (10) is employed [24]:

$$\begin{cases} \dot{x}_1 = x_2 & x_1(0) = x_{10} \\ \dot{x}_1 = u + f(x_1.x_2.t) & x_2(0) = x_{20} \\ y = x_1 \end{cases} \quad (10)$$

It is desired to reduce the order of this system to one, by defining the output tracking error: $e = y_c\,(t) - y(t)$, where y_c is desired output. A sliding surface is selected as:

$$S = \dot{e} + ke \qquad k > 0 \quad (11)$$

When the sliding variable S approaches zero, y (t) reaches y_c (t). If the disturbance magnitude has an upper-boundary, i.e. $|\,f\,| \le L$, u is designed as follows to drive $S \to 0$ in finite time and keep it at zero.

$$\begin{cases} u = w_1 + w_2 \\ w_1 = b\int sgn(S)dt \\ w_2 = c|S|^{\frac{1}{2}}sgn(S) \end{cases} \quad (12)$$

Where, $c = 1.5\sqrt{L}$ and b = 1.1 L. The super-twisting control (12) is continuous, since both terms are continuous [24]. The discontinues high-frequency switching term sgn(s) is 'hidden' under the integral. Figure 4 shows the block diagram of super twisting SMC, where, w_1 compensates the disturbance f in finite time, and w_2 forces S to become zero. This means that both e and $\dot{e}$ become zero, and the system trajectory stays on the surface thereafter. In other words, the control u drives e to zero, i.e. y approaches to y_c, in the presence of the bounded disturbance f.

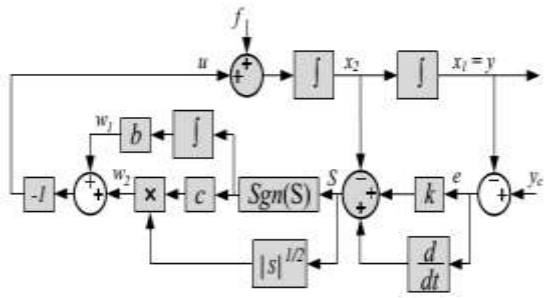

Fig. 4.Schematic control diagram of the super-twisting SMC

B. Proposed Super-twisting Sliding Mode DPC Strategy

The target of the proposed super-twisting SMC-DPC is to control PW active-power (P_p) and reactive-power (Q_p) independently and directly. In the proposed strategy, the CW voltage components, u_{dc} and u_{qc}, are the inputs to the system, whilst the power components P_p and Q_p are the outputs of the system, which are calculated as follows:

$$\begin{cases} P_p = -\frac{3}{2} Re\{\vec{u}_p{}^c \, \vec{i}_p{}^{c\,*}\} \\ Q_p = -\frac{3}{2} Im\{\vec{u}_p{}^c \, \vec{i}_p{}^{c\,*}\} \end{cases} \quad (13)$$

Where, $u^{\rightarrow}$ is space-vector of voltage and quantity Pp is positive if BDFIG is operating in the generator mode.

1) Sliding Surface

In order to minimize the steady-state error and make the transient response faster, instantaneous power errors are chosen as sliding surface:

$$S = [S_1 \quad S_2]^T \quad (14)$$

Where, $S_1 = P_{ref} - P_p$ and $S_2 = Q_{ref} - Q_p$. The surface S = 0 represent the accurate power tracking. When the system states reach and stay on the sliding surface, S = dS/dt = 0.

2) SMC Law

To derive conditions on the control law that will drive the system-states to the sliding surfaces, a candidate Lyapunov function is introduced:

$$w = \frac{1}{2} S^T S > 0 \quad (15)$$

Time derivative of the above Lyapunov function is calculated

$$\frac{dW}{dt} = \frac{1}{2}\left(S^T \frac{ds}{dt} + S\frac{ds^T}{dt}\right) = S^T \frac{ds}{dt} \quad (16)$$

According to (14), time derivative of S is given by:

$$\frac{ds}{dt} = \frac{d}{dt}\begin{bmatrix} S_1 \\ S_2 \end{bmatrix} = -\frac{d}{dt}\begin{bmatrix} P_p \\ Q_p \end{bmatrix} \quad (17)$$

To calculate time derivative of P_p and Q_p, we have

$$\left(\frac{d(\vec{u}_p{}^c \, \vec{i}_p{}^{c\,*})}{dt}\right) = \frac{d\vec{u}_p{}^c}{dt}\vec{i}_p{}^c * + \vec{u}_p{}^c \frac{d\vec{i}_p{}^{c\,*}}{dt} \quad (18)$$

The PWM voltage magnitude is considered constant, since it is connected to the grid, therefore

$$\vec{u}_p{}^c = \vec{U}_p e^{j(\omega_e - \omega_c)t} \quad (19)$$

The time derivative of PW voltage is:

$$\frac{d\vec{u}_p{}^c}{dt} = j(\omega_e - \omega_c)\vec{U}_p e^{j(\omega_e-\omega_c)t} = j(\omega_e - \omega_c)\vec{u}_p{}^c \quad (20)$$

Time derivative of the PW current is obtained from (5), (6) and (7),

$$\frac{d\vec{i}^c{}_p}{dt} = -\frac{L_m}{\sigma L'_p L'_c}\vec{u}^c{}_c + \left(\frac{r_c L_m}{\sigma L'_p L'_c} - j\frac{\omega_c L_m}{\sigma L'_p}\right)\vec{i}_c{}^c - \left(\frac{r_p}{\sigma L'_p} + \frac{j\omega_c}{\sigma}\right)\vec{i}_p{}^c + \frac{\vec{u}_p{}^c}{\sigma L'_p} \quad (21)$$

Equations (20) and (21) are substituted into (18), thus,

$$\frac{d(\vec{u}_p{}^c \, \vec{i}_p{}^{c\,*})}{dt} = \left[-\frac{r_p}{\sigma L'_p} + j\left(\omega_e - \omega_c + \frac{\omega_c}{\sigma}\right)\right]\vec{u}_p{}^c \, \vec{i}_p{}^{c\,*} - \frac{L_m}{\sigma L'_p L'_c}\vec{u}_p{}^c \, \vec{u}_c{}^{c\,*} + \left(\frac{r_c L_m}{\sigma L'_p L'_c} + j\frac{\omega_c L_m}{\sigma L'_p}\right)\vec{u}_p{}^c \, \vec{i}_p{}^{c\,*} + \frac{|\vec{u}_p{}^c|^2}{\sigma L'_p} \quad (22)$$

Equation (22) is decomposed to dq by using (13), According to (13), (17) and (23), time-derivative of sliding surface is obtained as:

$$\frac{ds}{dt} = F + DU^c{}_{cdq} \quad (23)$$

The switch control law is chosen based on super-twisting SMC [24] to make dW / dt < 0 for S ≠ 0. Thus, the following control law can be designed as:

$$U_{cdq}{}^C = -D^{-1}[F + U^*{}_c] \quad (24)$$

The required CW voltage vector $\boldsymbol{U}_{cdq}{}^c$ is generated by the SVM module.

3) Proof of the Stability

For stability in the sliding surfaces, dW/dt < 0 must be satisfied based on (16), (24) and (25):

$$\frac{dw}{dt} = -S(\int A sgn(S)\, dt + B|S|^{0.5} sgn(S)) \quad (25)$$

Where, S · sgn (S) > 0. Setting appropriate positive control gains yields dW/dt < 0. Since W is a positive-definite function and its time derivative (dW/dt) is a negative-definite function, S1 and S2 approaches zero asymptotically and the proposed controller becomes asymptotically stable.

4) Proof of the Robustness In practical application conditions, the performance of the control

system is impressed by system disturbances such as parameter variations, measurement noises, analogue-digital sample errors, thus, (24) can be rewritten as:

$$\frac{dS}{dt} = F + DU^{C}{}_{cdq} + H \quad (26)$$

Where $H = [H_1 \quad H_2]^T$,Thus

$$\frac{dw}{dt} = \frac{S^T dS}{dt} = -S(\int Asgn(S)\, dt + B|S|^{0.5} sgn(S) - H < 0 \quad (27)$$

If the positive control gains matrices A and B are set large enough to fulfill (28), dW/dt is still definitely negative. According to Lyapunov stability theorem, the proposed controller features strong robustness, if the control gains are selected properly.

$$|\int Asgn(S)\, dt + B|S|^{0.5} sgn(S)| > |H| \quad (29)$$

Fig. 5 shows the block diagram of the proposed SSMDPC. First, the measured PW voltages and currents, Upabc and Ip abc, are transformed into the dq stationary reference frame:

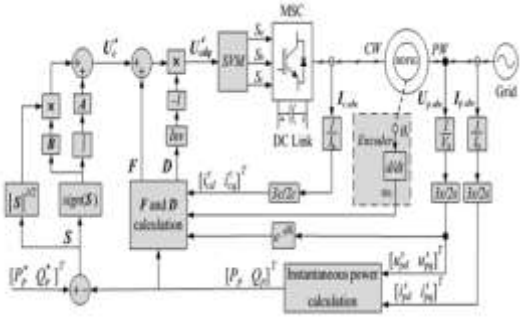

Fig. 5. A structural block diagram of the proposed SSM-DPC strategy control system for the inverter-fed BDFIG.

$U_{pdq}{}^{s}$ & $I_{pdq}{}^{s}$ Then, the PW active and reactive power can be calculated as follows:

$$\begin{cases} P_p = -\frac{3}{2}\{u_{dp}{}^{s} i_{dp}{}^{s} + u_{qp}{}^{s} i_{qp}{}^{s}\} \\ Q_p = -\frac{3}{2}\{u_{qp}{}^{s} i_{dp}{}^{s} - u_{dp}{}^{s} i_{qp}{}^{s}\} \end{cases} \quad (30)$$

Consequently, PW voltage $\boldsymbol{U}pdq\ s$ is transformed into the CW reference frame $\boldsymbol{U}\ pdq\ c$ and matrices F and D are obtained according to (24). In addition, errors of instantaneous active and reactive power of PW are used as the input of the super twisting SMC-based power controller. The CW voltage reference can be directly deduced in the CW reference frame, while, other presented SMC strategies use stationary reference frame and need reference frame transformation [15-17, 19-20]. The required CW voltage vector $\boldsymbol{U}_{cdq^c}$ is generated by space vector modulation (SVM) unit and it is worth noting that the proposed controller is simple and needs no synchronous coordinate transformations, PLL block and tuning PI parameters which makes such method favorable for the target application.

FUZZY LOGIC CONTROLLING

A block diagram about a fuzzy control system was shown within Fig. 6. Fuzzy controller was composed like following:

1. **A rule-base** (a set about If-Then rules), which contains a fuzzy logic output about linguistic description of achieving good control.
2. **An inference mechanism** (also called an "inference engine" or "fuzzy inference" module), which emulates decision making within interpreting & applying knowledge about how best toward controlling plant.
3. **A fuzzification interface**, which converts controller inputs into that inference mechanism can easily understand toward activate & apply rules.
4. **A defuzzification interface**, which converts conclusions about inference mechanism into actual inputs .

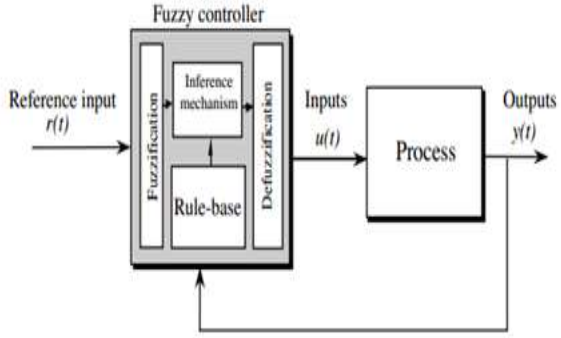

FIG.6. Fuzzy controller

The Membership functions about a fuzzy set was a speculation about pointer work within traditional sets. within fuzzy rationale, that speaks toward level about truth like an expansion about valuation. Participation capacities portray fuzziness (i.e. All data within fuzzy set), regardless about whether components within fuzzy sets were discrete or persistent.

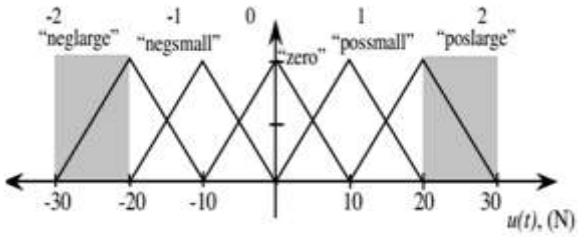

FIG.7. Membership functions

IV. SIMULATION RESULTS OF 2 MW BDFIG

In order to verify the proposed SSM-DPC strategy, for large machines, a 2 MW BDFIG is simulated in Matlab/Simulink® platform and the parameters of the generator are tabulated in Table I. During simulation, the sampling time and the simulation time-step were 100 μs and 5 μs respectively. The nominal speed of the investigated generator is 600 rpm which is considered as 1 pu. Since wind turbine inertia is large, the rotor speed variations are small and negligible [25]. Therefore, the simulation set-up evaluated considers the rotor speed constant, where by $\omega_m = 0.8$ pu.

TABLE I
3 kW and 2 MW BDFIG Parameters and Ratings

BDFIG	3 kW-Experimental	2 MW-Simulation
p_p, p_c	3, 2	3, 2
f_p, f_r (Hz)	50, 50	50,50
V_{pn}, V_{cn} (V_{rms})	380, 380	690, 690
r_p, r_c, r_r (Ω)	2.025, 0.96, 0.282	0.408, 1.186, 1.531
L_{lp}, L_{lc}, L_{lr} (mH)	11.9, 7.1, 19	0.014, 0.012, 0.026
L_{mp}, L_{mc} (mH)	260.7, 149.7	0.626, 0.373
S_b (kW)	3.9	2103.5
V_b (V_{rms})	$380/\sqrt{3}$	$690/\sqrt{3}$

The PW (Fig. 1) is connected to three-phase, 690 V_{rms}, and 50 Hz, where the nominal dc-link voltage of the machine side converter (MSC) is set to 1200 V and the dc capacitor is 16000 μF. The control parameters of the proposed SSM-DPC are tabulated in Table II. To evaluate performance and the effectiveness of the proposed SSM-DPC, comparative simulations involving DPC [11] and integral-SMC [13] strategies are investigated under the same conditions. Integral SMC in [13] is presented for DFIG, and is adopted for BDFIG. Switching frequency of the SSM-DPC and integral SMC strategies is set at 5 kHz.

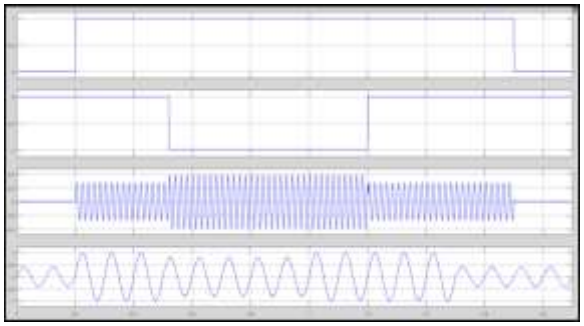

Fig. 8 Simulation results under step change conditions for active and reactive power with fuzzy based proposed method

TABLE II
Control Parameters of the Proposed SSM-DPC Strategy

BDFIG	A_1	A_2	B_1	B_2
2 MW-Simulation	100	35	7	6.5
3 kW-Experimental	4	20	2.2	8

Fig.8 gives the BDFIG response during different active and reactive power steps for the proposed method with fuzzy. The waveforms shown in Fig. 6 include PW active power, PW reactive power, PW phase current and CW phase current. Initially, PW active and reactive power references are set to zero. The PW active power is stepped from zero to 1 pu at t = 0 s and then backed to zero at t = 1.5 s, while the reactive power is stepped from zero to −1 pu at t = 0.5 s and backed to zero at t = 1 s.

The aforementioned comparative advancements show the accuracy and effectiveness of the proposed SSM-DPC during transient and steady-state conditions accordingly. Additional, simulation scenarios have been deduced and carried out to further evaluate the performance of the proposed SSM-DPC against rotor-speed variations, whereby the PW active and reactive powers are set to 1 pu and zero, respectively. The rotor speed is changed from 0.9 pu to 1.1 pu. Fig.9 shows that, during the speed variation, the PW active and reactive powers are controlled, whilst the CW current frequency initially decreases proportional to the BDFIG slip changes, reaching zero at the synchronous speed of 600 r/min, and increases after passing 600 r/min. Therefore, the proposed SSM-DPC has proven to be robust to rotor speed variations.

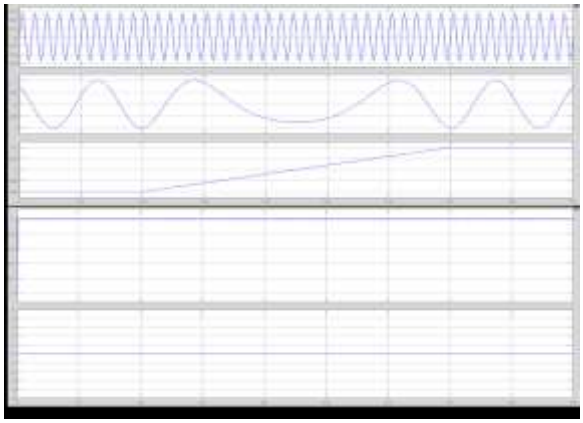

Fig. 9. Simulation results under rotor speed variation.

VI. CONCLUSION

This paper proposes an improved SSM-DPC strategy for the machine side converter of the BDFIG which controls both the active and reactive power independently. The proposed controller directly determines the required CW voltage based on the CW current, PW voltage, rotor speed, and values of active and reactive powers. The proposed method obtains the CW voltage in the CW-reference frame, outperforming the integral-SMC [13] which is very sensitive to the rotor-position error for transformation from PW to CW reference-frame.

However, the proposed method needs the rotor position and speed to calculate the control matrices F and D. Since the proposed SSM-DPC strategy is based on SMC method, it can be made robust to the effect of rotor position error in F and D by selecting appropriate gains for super-twisting mechanism. Simulation results on a 2 MW range and experimental results on a 3 kW BDFIG test rig have been provided and equated with those of DPC [11] and integral-SMC [13]. The main features of the proposed control system can be summarized as: - lower power ripple compared to integral-SMC and DPC, - less THD than integral-SMC and DPC strategies, due to its continuous controller output, - ability to control both active and reactive power directly without overshoot and with constant switching frequency, - provides excellent steady-state performance while having high transient response in contrast to DPC, - robustness against the machine parameters variation. Simulations and experimental tests have validated the effectiveness, robustness and feasibility of the proposed SSM DPC during numerous operating conditions (power transient changes and rotor speed variations) and machine parameter variations.

VII. REFERENCES

[1] G. Abad, J. López, M. Rodríguez, L. Marroyo and G. Iwanski, “Doubly fed induction machine: modeling and control for wind energy generation,” Wiley-IEEE Press, 2011.

[2] J. Carroll, A. McDonald and D. McMillan, “Reliability comparison of wind turbines with DFIG and PMG drive trains,” IEEE Trans. on Energy Conversion, vol. 30, no. 2, pp. 663-670, June 2015.

[3] J. Chen, W. Zhang, B. Chen and Y. Ma, “Improved vector control of brushless doubly fed induction generator under unbalanced grid conditions for offshore wind power generation,” IEEE Trans. on. Energy Conversion, vol. 31, no. 1, pp. 293-302, March 2016.

[4] P. Han, M. Cheng, Y. Jiang and Z. Chen, “Torque/power density optimization of a dual-stator brushless doubly-fed induction generator for wind power application,” IEEE Trans. on Ind. Electron., vol. 64, no. 12, pp. 9864-9875, Dec. 2017.

[5] P. Han, M. Cheng, X. Wei and Y. Jiang, “Steady-state characteristics of the dual-stator brushless doubly-fed induction generator,” IEEE Trans. on Ind. Electron., vol. 65, no. 1, pp. 200-210, Jan. 2018.

[6] K. Protsenko and D. Xu, “Modeling and control of brushless doubly fed induction generators in wind energy applications,” IEEE Trans. on Power Electron., vol. 23, no. 3, pp. 1191-1197, May 2008.

[7] G. Esfandiari, M. Ebrahimi and A. Tabesh, “Instantaneous torque control method with rated torque-sharing ratio for cascaded DFIMs,” IEEE Trans. on Power Electron., vol. 32, no. 11, pp. 8671-8680, Nov. 2017.

[8] S. Ademi and M. G. Jovanović, “Vector control methods for brushless doubly fed reluctance machines,” IEEE Trans., on Ind. Electron., vol. 62, no. 1, pp. 96-104, Jan. 2015.

[9] S. Ademi, M. G. Jovanović and M. Hasan, “Control of brushless doubly-fed reluctance generators for wind energy conversion systems,” IEEE Trans. on Energy Convers., vol. 30, no. 2, pp. 596-604, Jun. 2015.

[10] R. Sadeghi, S. M. Madani and M. Ataei, “A new smooth synchronization of brushless doubly-fed induction generator by applying a proposed machine

model," IEEE Trans. on Sustainable Energy, vol. 9, no. 1, pp. 371-380, Jan. 2018.

[11] J. Hu, J. Zhu and D. G. Dorrell, "A new control method of cascaded brushless doubly fed induction generators using direct power control," IEEE Trans. on Energy Convers., vol. 29, no. 3, pp. 771-779, Sept. 2014.

[12] C. Lascu, I. Boldea, and F. Blaabjerg, "Direct torque control of sensorless induction motor drives: a sliding-mode approach," IEEE Trans. on Ind. Appl., vol. 40, no. 2, pp. 582–590, Mar./Apr. 2004.

[13] J. Hu, H. Nian, B. Hu, Y. He and Z. Q. Zhu, "Direct active and reactive power regulation of DFIG using sliding-mode control approach," IEEE Trans. on Energy Convers., vol. 25, no. 4, pp. 1028-1039, Dec. 2010.

[14] G. Bartolini, L. Fridman, A. Pisano, and E. Usai, "Modern sliding mode control theory, new perspectives and applications," New York, NY, USA: Springer, 2008.

[15] M. I. Martinez, A. Susperregui1, and L. Xu, "Sliding-mode control of a wind turbine-driven double-fed induction generator under non-ideal grid voltages," IET Ren. Power Gen., vol. 7, no. 4, pp. 370–379, Jul. 2013.

[16] M. I. Martinez, G. Tapia, A. Susperregui, and H. Camblong, "Sliding mode control for DFIG rotor and grid-side converters under unbalanced and harmonically distorted grid voltage," IEEE Trans. on Energy Convers., vol. 27, no. 2, pp. 328–329, Jun. 2012.

[17] X. Wang, J. Yang, X. Zhang and J. Wu, "Sliding mode control of active and reactive power for brushless doubly-fed machine," ISECS Int. Colloquium on Computing, Communication, Control, and Management, Guangzhou, pp. 294-298, 2008.

[18] S. Z. Chen, N. C. Cheung, K. Chung Wong and J. Wu, "Integral sliding-mode direct torque control of doubly-fed induction generatorsunder unbalanced grid voltage," in IEEE Trans. on Energy Convers., vol. 25, no. 2, pp. 356-368, June 2010.

[19] F. Valenciaga and C. A. Evangelista, "2-sliding active and reactive power control of a wind energy conversion system," in IET Control Theory & Appl., vol. 4, no. 11, pp. 2479-2490, November 2010.

[20] C. A. Evangelista, A. Pisano, P. Puleston and E. Usai, "Receding horizon adaptive second-order sliding mode control for doubly-fed induction generator based wind turbine," IEEE Trans. on Control Syst. Techn., vol. 25, no. 1, pp. 73-84, Jan. 2017.

[21] G. Zhang, J. Yang, Y. Sun, M. Su, W. Tang, Q. Zhu and H. Wang, "A robust control scheme based on ISMC for the brushless doubly fed induction machine," in IEEE Trans. on Power Electron., vol. 33, no. 4, pp. 3129-3140, April 2018.

[22] C. Evangelista, P. Puleston, F. Valenciaga and L. M. Fridman, "Lyapunov-designed super-twisting sliding mode control for wind energy conversion optimization," in IEEE Trans. on Ind. Electron., vol. 60, no. 2, pp. 538-545, Feb. 2013.

[23] A. Chalanga, S. Kamal, L. M. Fridman, B. Bandyopadhyay and J. A. Moreno, "Implementation of super-twisting control: super-twisting and higher order sliding-mode observer-based approaches," in IEEE Trans. on Ind. Electron., vol. 63, no. 6, pp. 3677-3685, June 2016.

[24] Y. Shtessel, C. Edwards, L. Fridman, A. Levant, "Sliding mode control and observation," New York. Birkhäuser Boston, USA: Springer, 2014.

[25] D. Zhi and L. Xu, "Direct power control of DFIG with constant switching frequency and improved transient performance," IEEE Trans. on Energy Convers., vol. 22, no. 1, pp. 110–118, Mar. 2007.

[26] D. Zhi, L. Xu, and B. W. Williams, "Model-based predictive direct power control of doubly fed induction generators," IEEE Trans. on Power Electron., vol. 25, no. 2, pp. 341–351, Feb. 2010.